Electronic Structure Properties of Carbazole-like Compounds: Implications for Asphaltene Formation

I. García-Cruz,*,† J. M. Martínez-Magadán,† P. Guadarrama,‡ R. Salcedo,†,‡ and F. Illas†,§

Programa de Ingeniería Molecular, Instituto Mexicano del Petróleo, Eje Central Lázaro Cárdenas 152, Colonia San Bartolo Atepehuacan, México D. F., 07730, México, Instituto de Investigaciones en Materiales, Ciudad Universitaria, Universidad Nacional Autónoma de México, México, D. F., 04510, México, and Departament de Química Física i Centre especial de Recerca en Química Teòrica, Universitat de Barcelona i Parc Científic de Barcelona, Martí i Franquès 1, 08028 Barcelona, Spain

Received: July 18, 2002; In Final Form: December 3, 2002

A series of carbazole derivatives have been studied by means of ab initio density functional theory. The molecular structure of these compounds has been obtained by means of geometry optimization and characterized as potential energy surface minima. The analysis of the frontier orbitals together with the study of aromaticity permits one to make quantitative predictions about the reactivity of these molecules. This could be used to predict the influence of substituents on the chemical reactivity of carbazole-like moieties in asphaltenes.

I. Introduction

Asphaltene aggregation is a very serious problem in oil industry, with a huge economic impact. This is because asphaltene aggregation occurs spontaneously in the oil wells, leading to the formation of an extremely dense phase that impedes oil extraction and may even completely stop production.[1−10] Unfortunately, the mechanism of asphaltene aggregation is not known, and hence, it is difficult to design efficient strategies to avoid this undesirable process. To make this problem even more difficult, the structure of asphaltene species is to a large extent unknown. Zajac et al.[11] and, more recently, Groenzin and Mullins[12] have proposed some models, which, without pretending to exhaustively include all possible cases, are believed to be realistic representations of asphaltene molecules. Illustrative examples of these models are schematically depicted in Figure 1. However, it is important to point out that the mechanisms leading to the formation of the species represented in these models are also far from being well established. Several proposals exist in the literature aimed to explain the formation of asphaltene molecules. For instance, some authors suggest that asphaltene and other crude oil components are formed by disproportion of kerogen,[13] an insoluble large molecular weight material. It has also been proposed that asphaltene species can be formed by an oligomerization-like process involving a crude oil fraction containing a particular family of resins.[14,15] However, in the later case, the molecular mechanism leading to asphaltene formation and, in particular, the role played by the resins remain also unknown. Precisely, inspection of the asphaltene models depicted in Figure 1 suggests that these species contain a carbazole-substituted moiety. This particular family of resins may be seen as substituted carbazole-like molecules characterized by a pyrrolic ring symmetrically fused on both sides by two benzene rings (Figure 2).

The main idea here is to isolate the chemical effects derived from a given substitution in the carbazole moiety. However, one has to be aware that the π system of this moiety is effectively involved in the conjugation with the rest of the aromatic part of the asphaltene molecules. This prevents use of the carbazole moiety to extract information concerning long-range interactions such as electronic excitations. Yet, valuable information about the possible asphaltene formation oligomerization mechanism described in refs 14 and 15 can be acquired by a careful analysis of the molecular structure of carbazole and its derivatives. To this end, one needs to regard the carbazole derivative as embedded in the rest of the asphaltene in a way much similar to that used in surface science when representing graphite, silicon, or zeolites by a finite cluster model in which the dangling bonds are saturated by embedding hydrogen atoms.[16−21] Next, one can investigate the local properties of the carbazole moiety and, in particular, relevant reactivity indexes. First, one should keep in mind that carbazole-like molecules exhibit an aromatic character. Therefore, a proper reactivity index is the intrinsic aromaticity of the complete carbazole moiety; notice that the effect of a given substituent on the aromatic character of the substituted carbazole molecule affects the six-member rings as well as the pyrrolic ring. Another concept traditionally studied in connection with the concept of aromaticity is the inductive effect. Both aromaticity and inductive effects have been widely used in the study of the reactivity of related molecules.[22−24] With the above ideas in mind, the aim of this work is to study the aromaticity and inductive effect on several carbazole-type molecules. These include carbazole itself (CZ) and various derivatives, such as methyl carbazole (CZ−CH_3), hydroxyl carbazole (CZ−OH), bromide carbazole (CZ−Br), nitrile carbazole (CZ−CN), acetyl carbazole (CZ−$COCH_3$), (N−) unprotonated carbazole, and carboxyl carbazole (CZ−COOH). In addition, we have considered one additional compound having two substituents with different chemical character. This is the derivative containing one acetyl and one methyl, both on the same ring and in positions X (CH_3) and Y ($COCH_3$) as shown in Figure 2.

The aromaticity of these molecules has been analyzed in accordance with the nature of substituent groups and with the intrinsic inductive effect produced by the nitrogen atom coming from the central pyrrolic ring. Additionally, aromaticity changes

* Author to whom correspondence should be addressed. E-mail: igarcia@www.imp.mx.

† Instituto Mexicano del Petróleo.

‡ Instituto de Investigaciones en Materiales.

§ Departament de Química Física i Centre especial de Recerca en Química Teòrica.

10.1021/jp0216676 CCC: $25.00 © 2003 American Chemical Society
Published on Web 02/07/2003

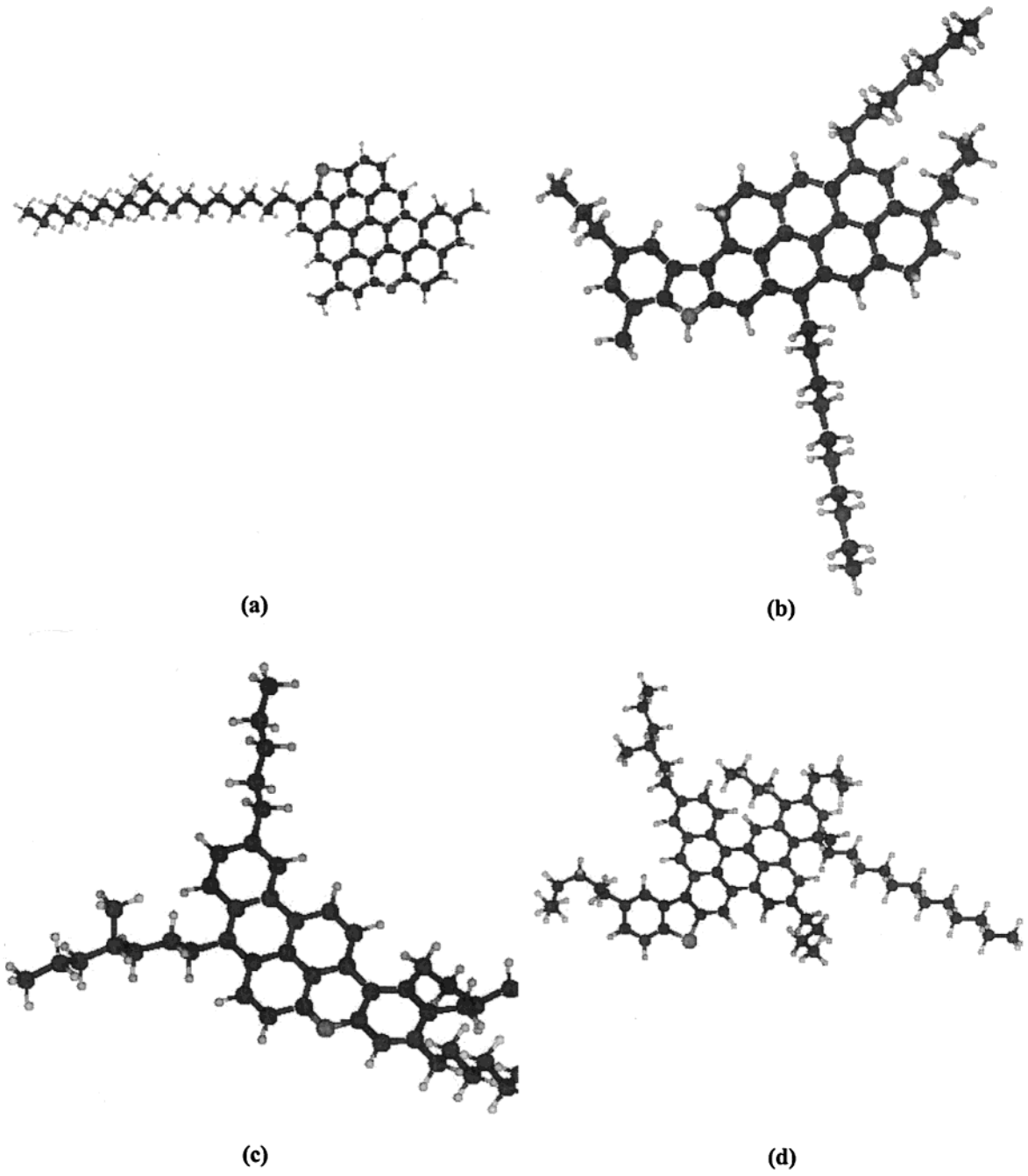

Figure 1. Asphaltene model as suggested in refs 11 (a) and 12 (b, c, and d)

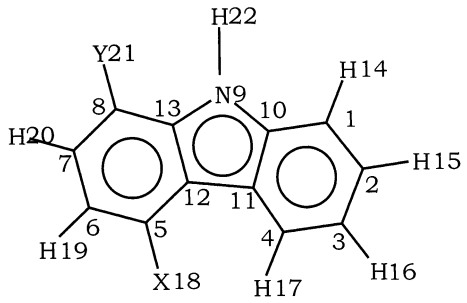

X= H, CH_3, OH, Br, CN, CH_3CO, COOH
Y= H, CH_3

Figure 2. Schematic representation of carbazole and the different substituted compounds used in this work**.**

due to the presence of substituent groups have been predicted and analyzed. These are supposed to be very useful for subsequent research about carbazole-containing resins and their role in the formation of the asphaltene phase. Finally, on the basis of the analysis of aromaticity as well as of frontier orbitals of the carbazole derivatives, some predictions about the reactivity of these molecules are made. In this sense, the present work has to be regarded as a step toward a theoretical understanding of the formation of these industrially relevant chemical compounds. To reach a firm conclusion about the molecular mechanism of asphaltene formation, additional work which is beyond the scope of the present research is required.

II. Computational Details

A careful structural study of carbazole and some carbazole derivatives has been carried out using ab initio quantum chemical techniques. This study aims to obtain reliable values for the various reactivity indexes described above. The electronic structure of the compounds in Figure 2 has been studied using

TABLE 1: Optimized Geometrical Parameters (Å and deg) of Carbazole Computed at Various Levels of Theory

parameter	B3LYP/6-31G** present work	B3LYP/6-31++G** present work	HF/6-31G* ref 35	MP2/6-31G* ref 35	B3LYP/6-31G* ref 35	X-ray ref 36
			bond length			
C_1-C_2	1.393	1.394	1.380	1.392	1.393	1.390
C_2-C_3	1.406	1.408	1.397	1.409	1.407	1.398
C_3-C_4	1.393	1.394	1.380	1.391	1.392	1.395
C_4-C_{11}	1.400	1.402	1.391	1.403	1.400	1.400
$C_{11}-C_{12}$	1.450	1.451	1.455	1.443	1.450	1.467
C_1-C_{10}	1.397	1.398	1.389	1.399	1.397	1.395
$C_{10}-C_{11}$	1.420	1.421	1.401	1.419	1.421	1.404
$C_{10}-N$	1.387	1.388	1.378	1.383	1.387	1.414
C_1-H	1.086	1.086	1.076	1.088	1.087	0.897
C_2-H	1.086	1.086	1.076	1.088	1.087	0.981
C_3-H	1.086	1.086	1.075	1.087	1.086	1.070
C_3-H	1.086	1.086	1.076	1.089	1.087	0.983
$N-H$	1.007	1.007	0.992	1.012	1.008	0.964
C_5-H	1.086	1.086				
			bond angle			
$C_1-C_2-C_3$	121.3	121.3	121.5	121.4	121.3	121.3
$C_2-C_3-C_4$	120.7	120.7	120.5	120.9	120.7	120.4
$C_3-C_4-C_{11}$	119.2	119.2	119.2	118.8	119.2	119.5
$C_4-C_{11}-C_{12}$	134.1	134.1	134.0	133.8	134.1	134.1
$C_1-C_{10}-C_{11}$	121.9	121.9	121.8	122.0	121.9	122.3
$C_2-C_1-C_{10}$	117.6	117.6	117.7	117.4	117.6	117.7
$C_4-C_{11}-C_{10}$	119.2	119.2	119.5	119.4	119.2	118.8
$C_{10}-C_{11}-C_{12}$	106.7	106.7	106.5	106.8	106.7	107.1
$C_{10}-N-C_{13}$	109.6	109.6	109.4	109.7	109.7	108.2
$C_{11}-C_{10}-N$	108.4	108.5	108.8	108.4	108.4	108.8
C_2-C_1-H	121.0	120.9	121.0	121.1	120.1	118.4
C_3-C_2-H	119.4	119.4	119.3	119.4	119.4	118.4
C_4-C_3-H	119.8	119.8	120.0	119.7	119.8	120.8
C_6-C_5-H	120.4	120.3	121.5	120.6	120.4	120.3

density functional theory within the well-known hybrid B3LYP method.[25] All geometries have been fully optimized with starting geometries obtained through the semiempirical PM3 approach.[26] The resulting geometries have always been characterized as true minima by vibrational analysis. Two basis sets of increasing accuracy have been used to determine the geometrical and electronic structure of these compounds. These are the 6-31G** and 6-31++G** standard basis sets, which include polarization and polarization plus diffuse functions, respectively. The B3LYP electronic structure calculations have been performed with the Gaussian 98 (G98) suite of computer programs,[27] whereas PM3 calculations have been carried out using the MOPAC package.[28]

Following von Ragué Scheleyer,[22] the nuclear independent chemical shifts (NICS) have been computed for the series of molecules given above in an attempt to quantify their aromatic character. The NICS are defined as the absolute magnetic shieldings computed at the ring center, which in turn is defined as the nonweighted average of the heavy atom coordinates. To have a correspondence with the familiar nuclear magnetic resonance (NMR) chemical shift convention, negative NICS denote aromaticity. The NICS have been calculated using the continuous set of the gauge transformation method,[29,30] within the B3LYP approach and basis sets used in the geometry optimization process. The NICS have been computed at the center of the six ring and pyrrolic rings. To complete the picture of the electronic structure of these compounds, the natural bond order (NBO) analysis[31−33] has also been carried out for all molecules studied in this work. The idea behind the NBO analysis is to use localized electron pairs, with each electron pair being a bonding unit and the charges derived from analysis of these units. Schematic representations of the molecular orbitals (MO) were obtained and analyzed by using the MOLDEN 3.4 program.[34]

III. Results and Discussion

III.a. Geometries. The molecules under study—carbazole, methyl carbazole, hydroxyl carbazole, bromide carbazole, nitrile carbazole, acetyl carbazole, anion carbazole, carboxyl carbazole, and 5methyl-8 acetyl carbazole—have been chosen on the basis of their different chemical activity. In fact, it is well known that methyl and hydroxyl derivatives (electron donor) activate ring aromaticity and act as ortho/para directors, whereas nitrile and acetyl derivatives (electron aceptor) deactivate aromatic rings and, furthermore, are meta directors on substitution. The Br (weak electron aceptor) derivative is a special case, because it weakly deactivates aromatic rings but acts as ortho/para director.

The optimized parameters for the carbazole molecule (Figure 2) calculated at the B3LYP/6-31G** and B3LYP/6-31++G** levels are displayed in Table 1, where previous values obtained at the HF/6-31G* and MP2/6-31G* levels[35] together with molecular parameters obtained from X-ray diffraction studies[36] are included for comparison. As expected, minimal differences appear in the structural parameters of carbazole when analyzing the B3LYP/6-31G** and B3LYP/6-31++G** results. The average variation in the distances is 0.001 Å, whereas changes in the bond angles are negligible. The calculated B3LYP/6-31G** and B3LYP/6-31++G** values are in very good agreement with experiment, with a slightly overestimated average distance of 0.004 Å with respect to the X-ray values[36] only and with bond angles also overestimated by ∼1 °. Notice that the present B3LYP/6-31++G** values are also in agreement with the MP2 values reported by Lee and Boo.[35]

Table 2 reports the ground state optimized parameters for carbazole and for the different derivatives considered in this work at the B3LYP/6-31++G** theory level. For the purpose of the present work and in the view of the previous discussion,

TABLE 2: Optimized Geometrical Parameters of Carbazole and Carbazole Derivatives Computed at the B3LYP/6-31++G Theory Level**

(a) Bond Lengths (Å)

parameter	CZ	CZ anion	CZ−CH_3	CZ−OH	CZ−Br	CZ−CN	CZ−$COCH_3$	CZ−COOH	CH_3−CZ−$COCH_3$
C_1-C_2	1.394	1.393	1.394	1.394	1.394	1.394	1.389	1.392	1.394
C_2-C_3	1.408	1.406	1.407	1.406	1.407	1.409	1.405	1.408	1.406
C_3-C_4	1.394	1.392	1.394	1.394	1.393	1.392	1.392	1.393	1.395
C_4-C_{11}	1.402	1.401	1.404	1.404	1.404	1.404	1.411	1.407	1.404
$C_{11}-C_{12}$	1.451	1.450	1.454	1.454	1.452	1.448	1.475	1.460	1.454
C_1-C_{10}	1.398	1.397	1.397	1.397	1.398	1.398	1.397	1.398	1.397
$C_{10}-C_{11}$	1.421	1.420	1.424	1.424	1.421	1.421	1.427	1.423	1.418
C_{10}−N	1.388	1.387	1.385	1.384	1.386	1.388	1.375	1.384	1.388
C_1−H	1.086	1.086	1.086	1.086	1.086	1.086	1.086	1.087	1.087
C_2−H	1.086	1.087	1.086	1.076	1.088	1.087	1.086	1.087	1.086
C_3−H	1.086	1.086	1.086	1.075	1.087	1.085	1.086	1.086	1.086
C_4−H	1.086	1.087	1.084	1.087	1.083	1.084	1.076	1.084	1.084
C_5−H	1.086	1.086							
$C_5-C(CH_3)$			1.506						1.507
C_5−O(OH)				1.369					
C_5−Br					1.906				
C_5−C(CN)						1.433			
$C_5-C(COCH_3)$							1.516		
C_5−C(COOH)								1.499	

(b) Bond Angle (deg)

parameter	CZ	CZ anion	CZ−CH_3	CZ−OH	CZ−Br	CZ−CN	CZ−$COCH_3$	CZ−COOH	CH_3−CZ−$COCH_3$
$C_1-C_2-C_3$	121.3	121.4	121.1	121.0	121.1	121.4	120.1	121.0	121.0
$C_2-C_3-C_4$	120.7	120.7	120.9	120.8	120.9	120.9	121.3	121.0	121.0
$C_3-C_4-C_{11}$	119.2	119.2	119.4	119.7	119.2	118.8	120.7	119.3	119.3
$C_4-C_{11}-C_{12}$	134.1	134.1	134.7	135.3	134.6	134.3	137.2	135.0	135.0
$C_1-C_{10}-C_{11}$	121.9	121.9	122.3	122.2	122.2	121.9	123.8	122.4	122.6
$C_2-C_1-C_{10}$	117.6	117.6	117.7	117.9	117.6	117.4	117.9	117.7	117.5
$C_4-C_{11}-C_{10}$	119.2	119.2	118.6	118.4	118.8	119.3	116.0	118.5	118.6
$C_{10}-C_{11}-C_{12}$	106.7	106.7	106.7	106.3	106.5	106.4	106.7	106.4	106.5
$C_{10}-N-C_{13}$	109.6	109.6	109.7	109.9	109.8	109.6	109.7	109.6	110.2
$C_{11}-C_{10}-N$	108.4	108.5	108.5	108.5	108.6	108.6	108.9	108.8	108.5
C_2-C_1-H	121.0	121.1	121.0	120.9	121.1	120.1	121.3	121.1	121.1
C_3-C_2-H	119.4	119.4	119.6	119.6	119.4	119.4	120.0	119.6	119.6
C_4-C_3-H	119.8	119.8	119.6	119.6	119.5	119.6	119.0	119.5	119.6
C_6-C_5-H	120.3	124.4							
$C_6-C_5-C(CH_3)$			120.8						120.6
$C_6-C_5-O(OH)$				117.4					
C_6-C_5-Br					118.5				
$C_6-C_5-C(CN)$						119.7			
$C_6-C_5-C(COH_3)$							119.0		
$C_6-C_5-C(COOH)$								116.5	

this level of theory can be considered as accurate enough. The isomer chosen for the substituted molecules is that where carbon atoms 4 or 5 are substituted (Figure 2). There are two reasons for this choice. First, as early as 1952 Dewar[37] showed that an electron-rich heteroatom such as nitrogen fused in a ring generates an orientation to a meta position, because of its tendency to withdraw electron density. In the present case, there are two possibilities, namely, carbon atoms 4 and 5 and 2 and 7. The second and chief reason is that the majority of known carbazole containing resins present their substitution precisely on carbon atoms 4 and 5. Therefore, this is the geometry used throughout this study. Upon substitution of the carbazole molecule, the main geometric features remain unchanged. This is found to be the case even for the unprotonated form of carbazole (Table 2). However, the electronic structure changes following the behavior expected from the presence of electron donor or electron acceptor substituents. The maximum difference in distance appears in the CZ−COCH3 moiety, where the C11−C12 bond is 0.024 Å larger than the corresponding value in CZ. Accordingly, the C4−C11−C12 bond angle exhibits the largest deviation—3 ° larger—with respect to the CZ molecule. Clearly, the most significant change in the distances is found in the bond C5−X18, since this corresponds to the position of the substitution.

TABLE 3: Total (*E*), HOMO and LUMO Energies, HOMO−LUMO Gap (Δ), and Dipole Moment (μ) of Carbazole and Carbazole Derivatives at B3LYP/6-31++G Theory Level**

molecule	E, (h)	HOMO (h)	LUMO (h)	Δ (eV)	μ (D)
CZ	−517.505519	−0.2117	−0.0403	4.66	1.66
CZ anion	−516.934755	−0.0282	0.0896	3.20	2.81
CZ−CH_3	−556.826342	−0.2085	−0.0362	4.69	1.32
CZ−OH	−592.729849	−0.2077	−0.0398	4.58	2.69
CZ−Br	−3088.634805	−0.2169	−0.0467	4.67	3.29
CZ−CN	−609.751272	−0.2278	−0.0710	4.26	6.16
CZ−$COCH_3$	−670.146544	−0.2194	−0.0725	3.99	4.74
CZ−COOH	−706.078965	−0.2284	−0.0694	4.32	6.75
CH_3−CZ−$COCH_3$	−709.480356	−0.2215	−0.0679	4.18	3.46

III.b. Electronic Properties. To discuss the electronic structure features of carbazole and its derivatives the total energy values, the HOMO−LUMO gaps are shown in Table 3 at B3LYP/6-31++G** level of theory. A schematic representation of these frontier orbitals is reported in Figures 3 and 4. For all molecules, the HOMO−LUMO gap remains in the 3.2−4.7 eV interval, even though important changes in the electronic structure exist,

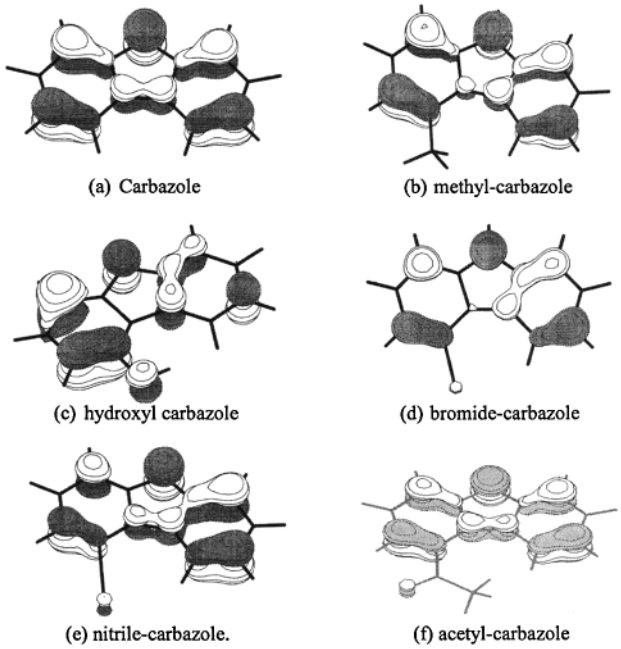

Figure 3. Schematic representation of the HOMO of carbazole derivatives.

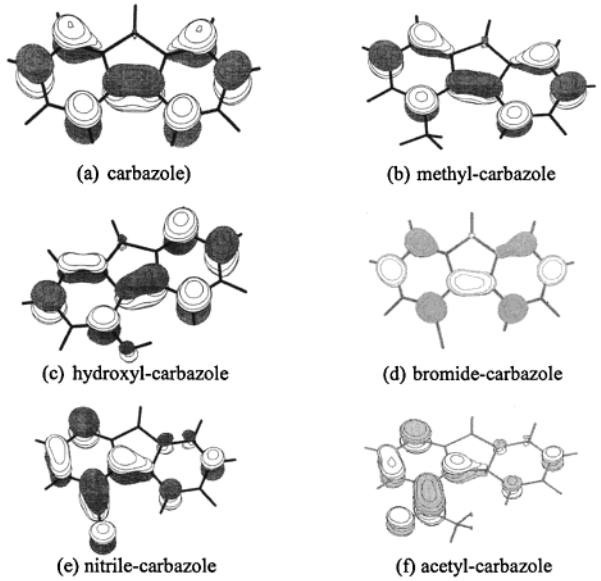

Figure 4. Schematic representation of the LUMO of carbazole derivatives.

which are induced by the presence of the different substituent groups. It is important to note that, for all these species, the HOMO−LUMO gap is within the experimental range for the onset of electronic absorption. In fact, for this kind of carbazole containing resins, fluorescence measurements[38,39] indicate a range of 3−5 eV for the absorption gap. Furthermore, the electrophilic character of the LUMOs is evidenced when the substituent is of electron acceptor nature (Figure 4). Hence, the smaller HOMO−LUMO gaps are found in the carboxyl-carbazole, nitrile-carbazole, and acetyl-carbazole, with the exception of the double substituted derivative and the carbazole anion. This is because in the former there is a strong influence of the acetyl substituent, whereas in the later, the negative charge destabilizes the HOMO with respect to that of the neutral molecule. The HOMO−LUMO gap is mainly governed by the LUMO, because the LUMO energies are considerably more affected by the presence of substituents than the HOMO ones.

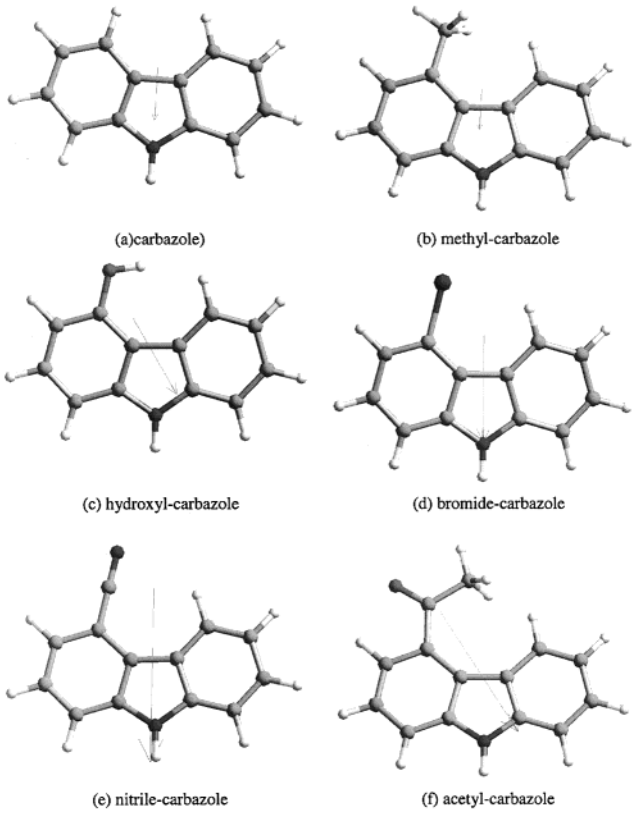

Figure 5. The dipole moment vector of carbazole and its derivatives.

This larger variation of LUMO energies is a result of the increased electron affinity in the molecules having electron acceptor substituents. The increase/decrease in electron affinity is parallel to the decrease/increase in ionization potential, but the effect is larger in the former, as expected. Hence, the LUMO of nitrile−carbazole and acetyl−carbazole are the ones with lowest energy (Table 3).

Another important property analyzed in the present work is the total dipole moment of each molecule obtained as the expectation value of the corresponding operator within the final B3LYP density. Relevant information about the dipole moments and on the variations of this observable quantity on carbazole derivatives induced by donor and acceptor substituents is also reported in Table 3. On one hand, the analysis of the module of the dipole moment already reveals rather large changes, which are a clear demonstration of the electron redistribution provoked by the presence of given substituent. However, a deeper insight may be reached by analyzing the orientation of the dipole moment vector. Figure 5 reports a schematic representation of the dipole moment vector with its origin placed at the center of mass of the corresponding molecule. From Figure 5, it is readily observed that donor groups such as methyl lead to a reduction of the dipole moment. Similarly, acceptor groups such as Br and nitrile groups largely enhance the dipole moment of the substituted carbazole molecule. These three substituents essentially affect the magnitude of the dipole moment. Interestingly enough, substituents with a more complex molecular structure also have a marked directional effect. This is the case for hydroxyl and acetyl derivatives; it appears that the presence of the oxygen atoms induces a rotation of the dipole moment vector.

The analysis of the dipole moments described above is consistent with the picture arising from the NBO analysis. This analysis is based in the electronic density of the whole molecule, and hence, it takes into account the effects of the σ-skeleton,

TABLE 4: Natural Bond Orbital Derived Charges of Carbazole[a]

atom	NBO//B3LYP/6-31G**	ref 8
C1	−0.277	−0.203
C2	−0.230	−0.164
C3	−0.265	−0.217
C4	−0.207	−0.133
C5	−0.207	−0.133
C6	−0.265	−0.217
C7	−0.230	−0.164
C8	−0.277	−0.203
N	−0.573	−0.330
C10	0.177	0.030
C11	−0.087	−0.081
C12	−0.087	−0.081
C13	0.177	0.030
H14	0.238	
H18	0.239	
H22	0.435	

[a] Mulliken charges from ref 8 are given for comparison.

of the π system including conjugation, and of the heteroatom. Results for carbazole molecule are included in Table 4 and compared to the results reported by Murgich et al.[3] also using DFT within a numerical basis set. In both cases, the N atom of the pyrrole ring appears to be the nucleophilic center, as expected. The larger NBO charge values indicate that one would expect the ortho and para positions with respect the nitrogen atom be favored for an electrophilic substitution in the homocyclic rings. However, these simple arguments neglect the inductive effect on the homocyclic ring caused by the fused ring. The fused rings have two connections with the homocyclic rings; the first one implies C13 and the heteroatom, and the second one is C12 and C11. In the first case, because of its pyrrolic nature, the N atom acts as an electron acceptor substituent, therefore favoring a meta orientation. In the second case, the C12 atom has an aromatic ring as substituent, this is an electron donor radical, and hence, it is expected to favor ortho/para substitution. In fact, this is an effect stronger than that caused by the heteroatom. The global result is the activation of C4 and C5 positions that are ortho to the C12 (or C11) and meta with respect to the nitrogen atom.

The majority of carbazole derivatives have precisely their substituents in the ortho and para positions, and this would indicate that the analysis of the carbazole molecule alone is enough to predict the most favorable substitute compound. The analysis of aromaticity of the different compounds permits one to further verify this assessment. The study of the aromaticity has been carried out in two steps. First, the intrisic aromaticity was measured, taking advantage of the NICS technique, and second, an estimate of the electron density has been made on the basis of the graphic shape of the resultant molecular orbitals. The results for the aromaticity are reported in Table 5. It is important to keep in mind that, at the B3LYP/6-311G** level, the NICS for benzene is −9.7 ppm.[22] In all cases, the calculated values have shown a clear and fairly interesting trend. In the case of carbazole, a very symmetric result emerges. The aromaticity on the two six-member rings is the same (−12.95 ppm) and is larger than that in the pyrrolic one (−10.24 ppm). The deprotonated carbazole anionic species has also been studied to analyze the behavior of an activated species derived from the neutral one, but without any chemical substitutions, the effect of a hypothetical electron donor group being simulated by the additional charge. The result is very interesting and illustrative of the adequacy of the NICS as as measure of aromaticity. In this species, the heterocycle nitrogen atom has a chemical environment and hybridization similar to that of pyridine; hence,

TABLE 5: Calculated Nuclear Independent Chemical Shifts (NICS) in ppm of Carbazole and Its Derivatives, As Obtained at the B3LYP/6-31++G Theory Level**

molecule	substituted ring	pyrrolic ring	nonsubstituted ring
CZ	−12.95	−10.24	−12.95
CZ anion	−12.02	−12.02	−12.02
CZ−CH_3	−13.09	−10.33	−12.81
CZ−OH	−13.97	−10.83	−13.35
CZ−Br	−13.31	−10.92	−13.85
CZ−CN	−12.95	−10.67	−13.32
CZ−$COCH_3$	−12.89	−10.61	−12.92
CZ−COOH	−12.78	−10.66	−13.10
CH_3−CZ−$COCH_3$	−12.98	−9.67	−12.07

it is expected that the aromaticity of the central ring will be enhanced by donor groups. In fact, this is found to be the case, and the NICS value for all three rings becomes −12.01ppm. This results in an effective average for the three rings. This situation should be carefully considered, because in these conditions, the nitrogen atom can participate in nucleophilic substitution reactions yielding quaternary salts. This will be further discussed in the next section, where a hypothetical asphaltene formation mechanism is discussed. In the methyl derivative, the NICS value on the substituted ring becomes −13.09 ppm and is of −12.81 ppm in the unsubstitued one. At first sight, this behavior seems to be strange, because one would expect that the inductive effect will lead to an increase on the aromaticity of the two six-membered rings. This case will be further commented on after discussion of the complete set of substituted carbazole molecules considered in the present work. The hydroxyl derivative exhibits an NICS value of −13.97 ppm on the substituted ring and −13.35 ppm on the free one. This is an expected behavior, because OH is a strong electronic donor group, leading to an important rise of the aromaticity, which is larger on the ring that receives the electronic donation. The Br derivative follows the trend discussed above for OH, with an increase of the NICS value of both rings with respect to carbazole: −13.31 ppm on the substituted ring, and −13.85 ppm on the free one. However, in this case, the NICS value is larger on the no-substituted ring, thus indicating that the substituted ring has been deactivated. This is a consequence of the large electronegativity of Br; the Br atom tends to withdraw electrons from the ring behaving as an inhibitor substituent with a concomitant decrease in the aromaticity of the substituted ring. The nitrile derivative has the classical behavior of an electron acceptor group. Because the NICS values are −12.95 ppm on the substituted ring and −13.32 ppm on the nonsubstituted one, the distribution is very similar to that on the Br derivative. The acetyl carbazole behavior is also similar to that of the nitrile and Br derivatives, with a value of the −12.89 ppm on the substituted ring and −12.92 ppm on the nonsubstituted ring. In the case of the carboxyl carbazole, the effect is the same as that found for the other cases having an electron acceptor susbtituent; the computed NICS values for the substituted and nonsubstituted rings are −12.8 and −13.1 ppm, respectively. A curious effect is found in the case of the acetate derivative, because the substitutent is chemically similar to that of the carboxyl derivative. However, in the former, the substitution on the ring takes place through the oxygen atom, and as a result the group has an activator effect; one finds −13.7 ppm for the substituted ring as compared to −12.9 ppm for the free one. The double substitution establishes, in practice, a competition between the two substituents and the one with deactivator effect, i.e., the acetyl group overcomes the methyl activator effect. The resulting values are −12.07 ppm for the substituted ring and

−12.98 ppm for the free one. In all cases, the pyrrolic ring presents an NICS average value of −10.7 ppm, lower than −15.1 ppm, which is that value calculated for free pyrrole.[23]

Overall, comparing the trend exhibited by the calculated NICS with carbazole is rather logical. However, the case of the methyl derivative exhibits a significant discrepancy. In this case, the calculated NICS in the nonsubstituted ring is the lowest in all carbazol derivatives. Indeed, this is the only case where this value decreases with respect to carbazole. A possible explanation of this, in principle, unexpected behavior can be the presence of hyperconjugation. This is supported by the NBO analysis: the net charge on C8 is −0.28, while that of C6 and C7 is −0.24. Notice that C8 is para with respect to C5, which is attached to the methyl substituent. Interestingly enough, the net charge on the carbon atom of the methyl group is −0.701. This picture suggests that there is an electronic accumulation on the C5 to C8 region, which may imply some olefinic character for C18. This is a rather clear indication of the presence of a hyperconjugative effect, which implies a complete rearrangement of the aromatic system. This is consistent with a +0.25 net charge on H23, H24, and H25, implying an increase of the acidity with respect of the other hydrogen atoms on the system.

V. Conclusions

Carbazole and several of its derivatives have been studied using ab initio density functional theory. The molecular structure of these compounds has been obtained by means of geometry optimization using analytical gradients. The resulting structures have been characterized as potential energy surface minima by pertinent vibrational analysis. For carbazole, the resulting geometry is in very good agreement with previous studies and with experiment.

The analysis of the frontier orbitals together with the study of aromaticity allows us to make quantitative predictions about the reactivity trends exhibited by carbazole derivatives, depending on the nature of the substituent. Some of these predictions could be anticipated from qualitative organic chemistry arguments. Nevertheless, the use of electronic structure arguments derived from ab initio calculations permits us to confirm or reject phenomenological hypotheses. For an electrophilic aromatic substitution, the hydroxyl derivative is found to be the most reactive compound of the family of compounds studied in the present work, whereas the nitrile-substituted compound is the molecule with the lowest activity. Judging from aromaticity measures based on the use of NICS, the methyl derivative seems to present an anomalous behavior. This is interpreted in terms of hyperconjugation. As expected, the Br derivative has ambiguous behavior. In the context of a nucleophilic reaction, the molecules with deactivant substituents that have accessible LUMOs are the most reactive.

The discussion above involved reactivity indexes which are essentially local in nature. Therefore, the electronic modifications induced by the presence of a given substituent in carbazole derivatives can be used to infer the reactivity of the carbazole moiety in asphaltenes, thus providing useful information about the chemistry of these important compounds and a step toward a theoretical understanding of the mechanism of asphaltene formation.

Acknowledgment. F.I. is grateful to the DURSI of the Generalitat de Catalunya and to the Spanish Ministerio de Ciencia y Tecnologia, project CICyT PB98-1216-CO2-01, for financial support.

References and Notes

(1) Speight, J. G. In *The Chemistry and Technology of Petroleum*, 3rd ed.; Marcel Dekker Inc.: New York, 1998.

(2) Tissot, B. P.; Welte, D. H. In *Petroleum Formation and Occurrence*; Springer-Verlag: New York, 1978.

(3) Murgich, J.; Abanero, J. A. *Energy Fuels* **1998**, *12*, 239.

(4) Buerostro-González, E.; Espinoza-Peña, M.; Andersen, S. I.; Lira-Galeana, C. *Pet. Sci. Technol.* **2001**, *19*, 299.

(5) Murgich, J.; Rodríguez, J. M.; Aray, Y. *Energy Fuels* **1996**, *10*, 68.

(6) Leon, O.; Contreras, E.; Dambakli, G.; Espidel, J.; Acevedo, S. *Energy Fuels* **2001**, *15*, 1028.

(7) Mansoori, G. J. *Pet. Sci. Technol. Eng.* **1997**, *17*, 101.

(8) Murgich, J.; Rogel, E.; León, O.; Isea, R. *Pet. Sci. Technol.* **2001**, **19**, 437.

(9) Carbognani, L.; Orea, M.; Fonseca, F. *Energy Fuels* **1999**, *13*, 351.

(10) Nalwaya, V.; Tangtayakom, V.; Piumsomboon, P.; Fogler, S. *Ind. Eng. Chem. Res.* **1999**, *38*, 964.

(11) Zajac, G. W.; Sethi, N. K.; Joseph, J. T. V. *Scanning Microsc.* **1994**, *8*, 463 1994.

(12) Groenzin, H.; Mullins, O. C. *Pet. Sci. Technol.* **2001**, *19*, 219.

(13) Durand B.; In *Kerogen Insouble Organic Matter From Sedimentary Rocks*; Durand, B., Ed.; Technip: Paris, 1980.

(14) Scotti, R.; Montanari, L. In *Asphaltenes, Fundamentals and Applications*; Sheu, E. Y., Mullins, O., Eds.; Plenum Press: New York, 2001.

(15) Mujica, V.; Nieto, P.; Puerta, L.; Acevedo, S. *Energy Fuels* **2000**, *14*, 632.

(16) Bagus, P. S.; Illas, F. The Surface Chemical Bond. In *Encyclopedia of Computational Chemistry*; Schleyer, P. V., Allinger, N. L., Clark, T., Gasteiger, J., Kollman, P. A., Schaefer, H. F., III, Schreiner, P. R., Eds.; John Wiley & Sons: Chichester, UK, 1998; Vol. 4, p 2870.

(17) Illas, F.; Sousa, C.; Gomes, J. R. B.; Clotet, A.; Ricart, J. M. In *Theoretical Aspects of Heterogeneous Catalysis, Progress in Theoretical Chemistry and Physics*, Chaer-Nascimento, M. A., Ed.; Kluwer Academic Publishers: Dordrecht, 2001; Vol 8, pp 149−181

(18) Casañas, J.; Illas, F.; Sanz, F.; Virgili, J. *Surf. Sci.* **1983**, *133*, 29.

(19) Pacchioni, G. *Heter. Chem. Rev.* **1995**, *2*, 213.

(20) Sauer, J. *Chem. Rev.* **1989**, *89*, 1999.

(21) Sauer, J.; Ugliengo, P.; Garrone, E.; Saunders, V. R. *Chem. Rev.* **1994**, *94*, 2095.

(22) Schleyer, P. v. R.; Maerker, C.; Dransfield, A.; Jiao, H.; Eikema-Hommes, N. J. R. v. *J. Am. Chem. Soc.* **1996**, *118*, 6317.

(23) Jiao, H.; Schleyer, P. v. R.; Mo, Y.; McAllister, A. M.; Tidwell, T. T. *J. Am. Chem. Soc.* **1997**, *119*, 7075.

(24) Cyrañski, M. K.; Krygowski, T. M.; Wisiorowski, M.; Eikema-Hommes, N.; Schleyer, P. v. R. *Angew. Chem., Int. Ed. Engl.* **1993**, *37*, 177.

(25) Becke, A. D. *J. Chem. Phys.* **1993**, *98*, 5648.

(26) Stewart, J. J. P. *J. Comput. Chem.* **1989**, *10*, 209.

(27) Frisch, M. J.; Trucks, G. W.; Schlegel, H. B.; Scuseria, G. E.; Robb, M. A.; Cheeseman, J. R.; Zakrzewski, V. G.; Montgomery, J. A., Jr.; Stratmann, R. E.; Burant, J. C.; Dapprich, S.; Millam, J. M.; Daniels, A. D.; Kudin, K. N.; Strain, M. C.; Farkas, O.; Tomasi, J.; Barone, V.; Cossi, M.; Cammi, R.; Mennucci, B.; Pomelli, C.; Adamo, C.; Clifford, S.; Ochterski, J.; Petersson, G. A.; Ayala, P. Y.; Cui, Q.; Morokuma, K.; Malick, D. K.; Rabuck, A. D.; Raghavachari, K.; Foresman, J. B.; Cioslowski, J.; Ortiz, J. V.; Stefanov, B. B.; Liu, G.; Liashenko, A.; Piskorz, P.; Komaromi, I.; Gomperts, R.; Martin, R. L.; Fox, D. J.; Keith, T.; Al-Laham, M. A.; Peng, C. Y.; Nanayakkara, A.; Gonzalez, C.; Challacombe, M.; Gill, P. M. W.; Johnson, B. G.; Chen, W.; Wong, M. W.; Andres, J. L.; Head-Gordon, M.; Replogle, E. S.; Pople, J. A. *Gaussian 98*, revision A.7; Gaussian, Inc.: Pittsburgh, PA, 1998.

(28) Stewart, J. J. P. *J. Comput. -Aided Mol. Des.* **1990**, *4*, 1.

(29) Keith, T. A.; Bader, R. F. W. *Chem. Phys. Lett.* **1993**, *210*, 223.

(30) Keith, T. A.; Bader, R. F. W. *Chem. Phys. Lett.* **1992**, *194*, 1.

(31) Foster, J. P.; Weinhold, F. *J. Am. Chem. Soc.* **1980**, *102*, 7211.

(32) Reed, A. E.; Curtiss, L. A.; Weinhold, F. *Chem. Rev.* **1988**, *88*, 899.

(33) Glendening, E. D.; Reed, A. E.; Carpenter, J. E.; Weinhold, F. *NBO, version 3.1*.

(34) Schaftenaar, G. *Molden 3.4*, CAOS/CAMM. The Netherlands, 1999.

(35) Lee, S. Y.; Boo, B. H. *J. Phys. Chem.* **1996**, *100*, 15073.

(36) Lahiri, R. N. *Acta Crytallogr.* **1969**, *25*, 127.

(37) Dewar, M. J. S. *J. Am. Chem. Soc.* **1952**, *74*, 3350.

(38) Groenzin, H.; Mullins, O. C. *J. Phys. Chem. A* **1999**, *103*, 11237.

(39) Groenzin, H.; Mullins, O. C. *Energy Fuels* **2000**, *14*, 677.